Toxicology in Vitro 106 (2025) 106058

Contents lists available at ScienceDirect

Toxicology in Vitro

journal homepage: www.elsevier.com/locate/toxinvit

The cyanobacterial toxins BMAA and 2,4-DAB perturb the L-serine biosynthesis pathway and induce systemic changes in energy metabolism in human neuroblastoma cells: A proteomic study

Lisa Pu [a], Joel R. Steele [b], Connor R. Phillips [a], Jake P. Violi [c], Kenneth J. Rodgers [a,*]

[a] Neurotoxin Research Group, School of Life Sciences, University of Technology Sydney, Ultimo, NSW 2007, Australia
[b] Monash Proteomics and Metabolomics Facility, Monash University, Melbourne, VIC 3800, Australia
[c] School of Chemistry, University of New South Wales, Sydney, NSW 2052, Australia

ARTICLE INFO

Editor Name: Dr. P Jennings

Keywords:
β-Methylamino-L-alanine
L-2,4-diaminobutyric acid
BMAA
DAB
Neurotoxins
Motor neuron disease
Amyotrophic lateral sclerosis
L-serine biosynthesis
Pyruvate
PHGDH

ABSTRACT

Blue-green algae (cyanobacteria), an ancient phylum of bacteria, produce a wide array of secondary metabolites that are toxic to humans. Rapid growth of cyanobacteria in an aquatic environment can result in algal blooms capable of turning waterways green and increasing toxin levels in the environment. Cyanobacterial toxins were first linked to the high incidence of a complex neurodegenerative disorder reported on the island of Guam in the 1940s but more recently have been linked to clusters of sporadic amyotrophic lateral sclerosis (sALS) worldwide. The non-protein amino acid β-*N*-methylamino-L-alanine (BMAA) and its isomer L-2,4-diaminobutyric acid (2,4-DAB) are produced concurrently by most cyanobacterial species. We carried out proteomic analysis on human neuroblastoma cells treated with BMAA and 2,4-DAB to determine the underlying mechanisms of toxicity resulting from exposure to these cyanotoxins and identified significant changes in the L-serine biosynthesis pathway as well as pathways associated with energy production in the cell such as fatty acid ß-oxidation and glycolysis. The impact on the serine biosynthetic pathway was supported by demonstrating a significant decrease in both mRNA and protein levels of the enzyme 3-phosphoglycerate dehydrogenase (PHGDH) the first committed step in serine biosynthesis. PHGDH uses 3-phospho-D-glycerate (3PG) an intermediate in the glycolytic pathway as a substrate, and co-incubation of cells with L-serine restored expression levels of PHGDH as did cell pre-treatment with the glycolytic product pyruvate. This is the first study to link exposure to BMAA and 2,4-DAB to impairments in the L-serine biosynthesis pathway and broad disturbances in energy metabolism.

1. Introduction

Cyanobacteria are an ancient, photosynthetic bacteria found on every continent (Büdel et al., 2016), and are capable of surviving in extreme environments (Cox et al., 2009; Sompong et al., 2005; Taton et al., 2006). Almost all cyanobacterial strains can produce a wide range of compounds that are toxic to humans (Dittmann et al., 2013) including the non-protein amino acid β-methylamino-L-alanine (BMAA) and its isomers L-2,4-diaminobutyric acid (2,4-DAB) and N-(2-aminoethyl) glycine (AEG) (Cox et al., 2005). BMAA is the most widely studied but often the least abundant isomer (Violi et al., 2019), and has been reported to cause oxidative stress, acute excitotoxicity (Weiss et al., 1989), protein aggregation (Dunlop et al., 2013), and ER stress (Main and Rodgers, 2018; Okle et al., 2013). 2,4-DAB can be up to 10-fold more abundant than BMAA (Violi et al., 2019) with a toxicity spectrum that includes excitotoxicity (Weiss et al., 1989), lathyrism (Ressler et al., 1961) and secondary ammonia toxicity in rats (O'Neal et al., 1968). When the toxicity of BMAA and its isomers were examined in mixed murine cortical cell cultures containing both neuronal and glial cells, AEG was found to be the most toxic isomer (Schneider et al., 2020). AEG toxicity was mediated by activation of mGluR5 receptors and induction of free radicals, while DAB acted at NMDA receptors (Schneider et al., 2020). Studies in undifferentiated human neuroblastoma cells that do not express mGLu5 or NMDA receptors (Kritis et al., 2015; Kulikov et al., 2007), reported that AEG was the least toxic of the BMAA isomers (Main and Rodgers, 2018).

The connection between BMAA and neurodegenerative diseases was first made on the island of Guam in the 1940s (Garruto et al., 1981; Reed

* Corresponding author.
E-mail address: Kenneth.Rodgers@uts.edu.au (K.J. Rodgers).

https://doi.org/10.1016/j.tiv.2025.106058
Received 18 November 2024; Received in revised form 6 March 2025; Accepted 26 March 2025
Available online 27 March 2025

et al., 1966) where the incidence of a neurodegenerative disease with features of amyotrophic lateral sclerosis (ALS), Parkinson's disease and Alzheimer's was reported to be 50 to 100 times that of the global population (Kurland and Mulder, 1954). Exposure to BMAA from the consumption of cycad flour and flying foxes that fed on cycad seeds, a local delicacy, was proposed as a trigger for the disorder (Banack et al., 2006; Cox et al., 2003; Whiting, 1963). BMAA in the seeds was synthesised by symbiotic cyanobacteria from the genus *Nostoc,* present in the roots of the cycads (Cheng and Banack, 2009; Polsky et al., 1972). There is substantial evidence that the high incidence of ALS/PDC on Guam was related to lifestyle factors that rapidly changed with Westernisation of the inhabitants of the island due to the presence of the American naval base (reviewed in (Rodgers et al., 2018)). The arrival of firearms to the island decimating the flying fox population which were part of the Chamorro diet (Banack and Murch, 2009). The change in lifestyle, and in particular diet, therefore, is likely to have resulted in the decrease in the incidence of ALS/PDC. This contrasts with the increased incidence of ALS/MND that has been reported in some countries over the past few decades and coincides with an increased incidence of BGA blooms (Koreivienė et al., 2014).

An early study in macaques showed that orally administered BMAA resulted in motor neuron dysfunction, supporting the proposed link between BMAA and neurological disease (Spencer et al., 1987). A more recent study in which vervets were fed BMAA (210 mg kg^{-1} d^{-1}) for 140 days identified an increase in neurofibrillary tangles (NFTs) and β-amyloid deposits in brains of BMAA-dosed vervets which were reduced in abundance when the animals were co-fed with L-serine (Cox et al., 2016). BMAA caused degeneration of the upper and lower motor neurons, activated microglia, and induced proteinopathies with reactive astrogliosis in the anterior horns of the spinal cord of the vervets (Davis et al., 2020). There was a reduction in the BMAA-triggered pathological changes on coadministration of L-serine (Davis et al., 2020).

The first link between L-serine and BMAA was reported in an *in vitro* study demonstrating that co-administration of L-serine reduced levels of radiolabelled BMAA in proteins and decreased the amount of autofluorescent bodies in BMAA-treated cells (Dunlop et al., 2013). L-serine was subsequently shown to protect against BMAA-induced proteotoxic stress *in vitro* (Main et al., 2016), and to reduce BMAA-induced electrophysiological impairment in rats (Cai et al., 2018). In vervet studies, levels of BMAA in proteins did not change in the presence of L-serine despite L-serine having a neuroprotective effect (Cox et al., 2016), so while these studies supported an interaction between BMAA and L-serine, the mechanisms involved were not clear. Indeed, studies with isolated enzymes showed that BMAA is a substrate for human alanyl-tRNA synthetase (HsAlaRS), rather than seryl-tRNA synthetase and is not subject to the HsAlaRS intrinsic proofreading activity allowing 3.5 % of active $tRNA^{Ala}$ to be charged with BMAA (Han et al., 2020). BMAA can inhibit both the activation and editing catalytic efficiency of HsAlaRS (Han et al., 2020).

L-serine is classified as a conditionally-essential amino acid and can be derived from four sources: dietary intake, biosynthesis, recycling, and directly from L-glycine (de Koning et al., 2003). However, *de novo* synthesis of L-serine accounts for 73 % of all L-serine sources in humans (Kalhan and Hanson, 2012) and it is the precursor to other amino acids such as L-glycine and L-cysteine which are both used in the formation of the antioxidant glutathione. Furthermore, L-serine is the dominant source of one-carbon groups for purine synthesis where the purines generated are further used in various methylation reactions (de Koning et al., 2003). L-serine can be taken up from the extracellular space by amino acid transporters or synthesised *de novo via* the phosphoserine pathway (Reid et al., 2018). 3-phosphoglycerate dehydrogenase (PHGDH) is the first enzyme in the phosphoserine pathway. PHGDH knock-out mice display severe brain malformation and die after embryonic day thirteen (Metcalf et al., 2018), highlighting the absolute necessity of L-serine, synthesised *de novo* for nervous system development and health. The neuroactive substance D-serine is produced from the isomerisation of L-serine in neurons (de Koning et al., 2003) and in addition, L-serine serves as a building block for phosphatidylserine and sphingolipids, both of which are important components of the plasma membrane (de Koning et al., 2003). Patients suffering from PHGDH deficiencies displayed several neuropathologies which were only modestly improved by L-serine supplementation, suggesting *de novo* synthesis of L-serine is required for proper neuro-function and development (Jaeken et al., 1996). Neurons, in particular, are largely dependent on the L-serine biosynthesis pathway since L-serine is not readily transported across the blood brain barrier, thus defects or downregulation of enzymes involved in the biosynthetic pathway would have pronounced detrimental effects on the brain (Smith et al., 1987).

Despite the fact that BMAA and its isomers are almost always found together in nature making human exposure to BMAA alone unlikely, only a few studies have investigated the toxicity of cyanotoxin mixtures (Main and Rodgers, 2018; Martin et al., 2022; Martin et al., 2019). While Main did not find a synergistic increase in the general toxicity for the combined treatments when compared to the single treatments, caspase-3 activity, lysosomal protease activity and ER stress markers were significantly increased in the BMAA and 2,4-DAB combination when compared to the single treatments (Main and Rodgers, 2018). A simplex axial mixture study performed by Martin using NSC-34 cells found that equimolar concentrations of BMAA, 2,4-DAB and AEG resulted in the highest decrease in cell viability and highest caspase-3/7 activity (Martin et al., 2019). A follow-up study using the same experimental design in zebrafish showed that 2,4-DAB resulted in the lowest viability, lower than any of the combinations with toxic load taken into account (Martin et al., 2022). In the present study, we examined proteomic changes in neuroblastoma cells exposed to BMAA and 2,4-DAB. Given the ability of L-serine to protect cells and organisms against BMAA toxicity, and its central role in CNS function, we followed up on the changes identified in the enzymes involved in the L-serine biosynthesis pathway using western blotting and RT-qPCR.

2. Materials & methods

2.1. Reagents and chemicals

Dulbecco's Modified Eagle's Medium (DMEM) high glucose (D5796), DMEM high glucose with sodium pyruvate (D6546), Minimum Essential Medium Eagle (EMEM) (M2279) and BMAA were purchased from Sigma Chemical Co., St. Louis, MO. 2,4-DAB was purchased from Toronto Research Chemicals, Toronto, ON.

2.2. Cell culture

Undifferentiated SH-SY5Y human neuroblastoma cells (American Tissue Culture Collection, catalogue number CRL-2266) passage 19–24 were maintained in DMEM supplemented with 10 % heat-inactivated foetal bovine serum (FBS) (Australia origin, Sigma Chemical Co.) and 2 mM GlutaMAX (Thermo Fisher Scientific, Waltham, MA, USA) at 37 °C with 5 % CO_2. Cells were treated with BMAA and 2,4-DAB in EMEM media which does not contain L-serine.

2.3. Viability measures of BMAA and 2,4-DAB treated SH-SY5Y cells

Cells were seeded at 30,000 cells/well in 96-well plates in DMEM and allowed to adhere overnight. Stock solutions of 80.4 mM BMAA and 84.6 mM 2,4-DAB were made in ultrapure water. Working solutions of 2 mM were prepared from stock solutions in EMEM media and added to the cell cultures to give the final concentrations indicated in Table 1. Treatment was performed with four replicates of the concentrations of BMAA and 2,4-DAB shown in Table 1. Cells were treated for 48 h before incubating with 10 % AlamarBlue (Thermo Fisher) for 2 h at 37 °C, with 5 % CO_2. Fluorescence was read at 570 nm for excitation and 585 nm for emission. Fluorescence was normalised to the amount of protein in each

Table 1
Final concentrations of BMAA and 2,4-DAB used in the cell viability assays.

	BMAA (μM)	2,4-DAB (μM)
Single treatments	125	
	250	
	500	
	1000	
		125
		250
		500
		1000
Combined treatments	50	500
	100	1000
	500	500
	500	50
	1000	100

well as determined by the bicinchoninic acid (BCA) assay.

2.4. Proteomic investigation of SH-SY5Y neuroblastoma cells exposed to equimolar concentrations of BMAA and 2,4-DAB

SH-SY5Y cells were treated at 80 % confluency in 175 cm^2 flasks for 48 h with 500 μM BMAA plus 500 μM 2,4-DAB ($n = 3$). Cell pellets were snap frozen in liquid nitrogen and stored at −80 °C prior to analysis. Cells were lysed in lysis buffer (20 mM HEPES, pH 7.4, 1 % Triton X-100, 1 mM EDTA) containing a protease and phosphatase inhibitor cocktail (10 μg/mL aprotinin, 10 μM leupeptin, 1 mM PMSF, 1 mM $NaVO_3$, 100 mM NaF, 1 mM Na_2MoO_4 and 10 mM $Na_4P_2O_7$). Samples were probe sonicated three times at 50 Hz for 15 s with 20 s between each pulse. Insoluble matter was removed by centrifugation at 15,000 ×*g*, 4 °C for 10 min. The supernatant was transferred into new tubes and proteins were reduced with 5 mM DTT for 15 min at room temperature and alkylated with 10 mM iodoacetamide for 30 min at 4 °C shielded from light. The alkylation reaction was then quenched with an additional 5 mM DTT for 15 min. Detergents and contaminants were removed using a chloroform-methanol precipitation protocol (Wessel and Flügge, 1984). The protein pellet was resuspended in 200 μL of 8 M Urea in 50 mM Tris (pH 8.8). A BCA protein assay (Pierce, Rockford, USA) was performed and 150 μg of protein was used in a dual digestion process with Lys-C at a 1:100 enzyme to protein ratio overnight at room temperature and then with trypsin at a 1:100 enzyme to protein ratio for at least 4 h at 37 °C. Peptides were acidified with a final concentration of 1 % trifluoroacetic acid (TFA) (pH 2 to 3) and purified using SDB-RPS 3 M-Empore stage tips (Humphrey et al., 2018).

A 10plex TMT experiment was performed. The dried peptides were resuspended in 200 mM HEPES (pH 8.2) and peptide concentrations were measured with a MicroBCA protein assay kit (Thermo Scientific, Rockford, IL). TMT labelling was performed with 0.2 mg of 20 μL reagent with 70 μg of sample peptides. Labelling was performed at room temperature for an hour. The TMT reaction and reverse tyrosine labelling were stopped with 8 μL of 5 % hydroxylamine per sample, followed by vortexing and incubation at room temperature for 15 min. Samples were combined, dried with vacuum centrifugation, fractionated with basic reverse phase (RP) isocratic step elution with RP spin columns (Pierce) and loaded onto RP cartridges. Elution was performed with 10 mM ammonium bicarbonate using 12 fractionation steps with the following acetonitrile (ACN) concentrations: 5, 10, 12.5, 15, 17.5, 20, 22.5, 25, 27.5, 30, 40, 80 % ACN. These fractions were then pooled into six subsets (fractions 1–7, 2–8, 3–9, 4–10, 5–11, 6–12) and were dried and desalted using SDB-RPS 3 M-Empore stage tips.

2.5. Analysis of the proteome

Fractionated peptides were reconstituted in 30 μL of 0.1 % formic acid (FA) and 10 μL of the samples were analysed on an Orbitrap Fusion Tribrid-MS (Thermo Scientific) equipped with a UHPLC Proxeon chromatography system. The peptides were separated with a gradient from 6 to 30 % ACN with 0.125 % FA at a flow rate of 400 nL/min for 3 h. Each survey full scan (400–1400 *m/z*) was acquired in the Orbitrap (with 120,000 resolution, at 400 m/z, AGC of 2×10^5). MS3 fragmentation was performed using higher-energy collisional dissociation (HCD) with 55 % collision energy and reporter ion detection of 150,000 ions with AGC, 60,000 resolution and maximum ion accumulation time of 150 ms in the Orbitrap. Peptide fragmentation and reporter ion spectra collection were performed using the synchronous precursor selection method (McAlister et al., 2014). In this method, the 10 most intense ions were isolated and MS2 analysis was performed using CID fragmentation with the following settings: normalised collision energy of 35 %, 4×10^3 AGC, 0.5 Da isolation window and maximum ion accumulation time of 150 ms with 40 s of dynamic exclusion. Post MS2 scan, precursor isolation was performed for MS3 analysis using a 2.5 Da window and fragmented in the ion trap with the same CID settings as above, except with an AGC setting of 8000. Multiple fragment ions (or sequential precursor selection (SPS) ions) were isolated and then fragmented by HCD with a normalised collision energy of 37.5 %. Fragmented ions were selected based on the previous MS2 scan. MS2-MS3 was conducted using the SPS methodology (McAlister et al., 2014).

The data were analysed as per an in-house constructed pipeline previously described (Mirzaei et al., 2017a). Briefly, the raw data files were converted to mzXML and erroneous charge states and monoisotopic m/z values were corrected using a published method (Huttlin et al., 2015). MS/MS spectra were assigned sequences using the Sequest algorithm (Eng et al., 1994) with searches performed against the human SwissProt Uniprot database. Data searches were performed using cysteine carbamidomethylation and TMT on the N-terminal of peptides, lysine residues as static modifications and oxidation of methionine as dynamic modifications (20 ppm precursor ion tolerance, 0.8 Da fragment ion tolerance for CID). Sequest matches were filtered using linear discriminant analysis applied to a false discovery rate (FDR) of 1 % at the peptide level based on matches to reversed sequences, as reported above (Eng et al., 1994). Quantification of peptides using TMT reporter ions was conducted with an established method (McAlister et al., 2012). Proteins were regarded as changing in abundance based on a two-sample *t*-test $p < 0.05$ and fold change threshold of >1.3 for increased abundance and < 0.77 for decreased abundance. Pathway enrichment analysis was carried out on proteins significantly changing in abundance using Ingenuity Pathway Analysis (IPA) software (Ingenuity® Systems, www.ingenuity.com). Identified proteins were matched to corresponding genes using the Ingenuity Pathway Knowledge base (IPKB) with interaction networks ($p > 0.05$) and molecular and cellular ontology based on known protein-protein interactions in published literature (curated knowledge base). Networks were identified on the most common functional groups present. Canonical pathway analysis was used to identify function-specific genes that are significantly present within the networks.

2.6. RT qPCR to determine L-serine biosynthesis enzyme expression levels

SH-SY5Y cells were maintained in DMEM, or DMEM with 0.11 g/L sodium pyruvate supplementation before treatment. Cells were treated at 70 % confluency in triplicate 25 cm^2 flasks for 48 h with 500 μM BMAA, 500 μM 2,4-DAB and 500 μM BMAA plus 500 μM 2,4-DAB in EMEM. Cell pellets were washed three times with PBS. During the final wash, each sample was aliquoted in half, centrifuged at 800*g* with the supernatant removed afterwards. The remaining cell pellet was then stored at −80 °C for western blotting while the other half proceeded to RT qPCR.

RNA was isolated using TRI reagent and quality checked using the Nanodrop 1000 (Thermo Fisher) and with a bleach gel (Aranda et al., 2012) before proceeding to cDNA synthesis. 1 μg of RNA was reversed transcribed using the Tetro cDNA synthesis kit from Bioline. RT qPCR was performed using the Bio-Rad CFX96 Real-Time System coupled with

a C1000 Thermal Cycler. 15 ng of cDNA was used with the SensiFAST™ SYBR® No-ROX kit (Bioline) and duplicate technical replicates were averaged during statistical analysis. The experiment was repeated three times for a total of $n = 9$.

Custom primers were designed using NCBI Primer-BLAST, MFE-primer 3.0 and Oligo analyser and synthesised by Sigma (Table 2). Post-run analysis was performed using Bio-Rad CFX Manager and fold change was calculated using the $2^{-\Delta\Delta CT}$ method (Livak and Schmittgen, 2001) and normalised to the housekeeping gene glyceraldehyde 3-phosphate dehydrogenase (GAPDH). A melt curve analysis was performed to ensure there was no RNA degradation and to check for primer specificity.

2.7. RT qPCR of BMAA and L-serine treated SH-SY5Y cells

SH-SY5Y cells were seeded into 6-well plates at 280,000 cells per well in DMEM and left to adhere overnight. Treatment was performed with nine replicates of the following concentrations: 500 μM BMAA plus 50 μM L-serine, 500 μM 2,4-DAB plus 50 μM L-serine and 500 μM BMAA plus 500 μM 2,4-DAB plus 100 μM L-serine. After 48 h of treatment, cells were washed thrice with PBS. 1 mL of TRI reagent was then added and aspirated several times to ensure cell lysis before being transferred into tubes. RNA was isolated using TRI reagent from Sigma as per the manufacturer's guidelines. cDNA synthesis and RT qPCR were performed as previously described.

2.8. Western Blots of PHGDH protein

RIPA lysis buffer (25 ml, Thermo Fisher Scientific) was mixed with half a tablet of protease inhibitor cocktail (Roche, Basel, Switzerland) and 110 μL added to each sample tube. Samples were probe sonicated twice on ice at 40 % power for 30 s using the Qsonica Q125 sonicator. The lysates were then centrifuged at 10,000*g* for 10 min. 10 μL of the lysate was used for protein quantification (BCA assay).

Three parts of the sample were mixed with one part of Laemmli buffer (4 times concentrate), heated at 85 °C for 5 min and centrifuged at 10,000*g* for 5 min to remove any insoluble proteins. A total of 45 μg protein was then loaded into a Novex™ WedgeWell 10–20 % Tris-Glycine gel with 10 μL of SeeBlue® Plus2 Pre-Stained Protein Standard ladder loaded in the first lane. The gel was left to run at 225 V for 40 min before being wet transferred onto an Amersham™ Hybond ECL nitrocellulose 0.45 μm membrane (Amersham Biosciences, Buckinghamshire, UK) at 20 V for 1 h. Membranes were immersed in Ponceau S (Sigma-Aldrich) for 5 min to check for transfer quality and blocked overnight with 5 % non-fat milk in PBS-T at 4 °C with constant agitation. Primary monoclonal antibodies were diluted at 1:15,000 and 1:1500 in PBS-T for beta-actin (Cat. No. BLR057F Abcam, Melbourne, Victoria) and PHGDH (Cat. No. 66350 Cell Signaling Technology, Danvers, MA) respective and membranes incubated for 1 h at room temperature separately per primary antibody. Membranes were then incubated in the secondary antibody goat anti-rabbit IgG peroxidase (Cat. No. A6154 Sigma-Aldrich) diluted 1:6000 in PBS-T for 1 h at room temperature and imaged with Clarity™ Western ECL Substrate (Bio-Rad, Hercules, CA) on an Amersham Imager 600. Band intensity was analysed with the software on the Amersham Imager 600 and the target protein was normalised to the housekeeping protein, beta-actin.

2.9. Bicinchoninic acid assay for protein normalisation

Following the AlamarBlue assay endpoint, the reagent was removed from the wells and the cells were washed three times with phosphate buffered saline (PBS). 50 μL of 0.02 % Triton™ X-100 (Sigma-Aldrich, Castle Hill, NSW, Australia) was added to each well and the plate was freeze-thawed at −80 °C. A solution consisting of 4 % (*w/v*) copper (II) sulphate ($CuSO_4$) and BCA solution purchased from Sigma-Aldrich was mixed in a 1:50 ratio and 100 μL was added to each well. The plate was covered and left to incubate for 30 min at room temperature before being read on the Tecan Infinite M1000 pro at an absorbance wavelength of 562 nm. Cell viability values were then normalised to the protein absorbance values.

2.10. Statistical analysis

TMTPrepPro script, was utilised for the statistical testing of proteomic data which is custom based R scripts developed by Mirzaei (Mirzaei et al., 2017b). Statistical tests on viability, RT-qPCR and western blotting data were performed on Prism software (GraphPad software, CA, USA) using one-way ANOVA and the post-hoc tests indicated in the figure legends (Sidak's or Dunnett's).

3. Results

3.1. Viability of SH-SY5Y cells was significantly reduced when cells were exposed to 2,4-DAB but exposure to BMAA resulted in no changes in cell viability

Cell viability was estimated from the reduction of resazurin to resorufin in metabolically active cells (AlamarBlue®). There was no significant change in viability with increasing concentrations of BMAA (Fig. 1A). A significant decrease in cell viability was observed with 2,4-DAB at the higher concentrations examined (Fig. 1B); 500 μM ($P < 0.001$) and 1000 μM ($P < 0.0001$).

3.2. Combined treatment of SH-SY5Y cells with BMAA and 2,4-DAB resulted in a significant decrease in cell viability

When cell viability was assessed using the AlamarBlue® reagent, all the combinations of BMAA and 2,4-DAB examined significantly reduced cell viability relative to untreated cells (Fig. 2). Equimolar concentrations of 500 μM BMAA and 500 μM 2,4-DAB resulted in the lowest cell viability ($P < 0.0001$). Equimolar concentrations of BMAA and 2,4-DAB were used in subsequent studies to examine proteomic changes in the cells. Despite not being toxic individually at concentrations of 500 μM BMAA and 50 μM 2,4-DAB when combined there was a significant reduction in viability.

Table 2
Primers for 3-phosphoglycerate dehydrogenase (PHGDH), phosphoserine aminotransferase 1 (PSAT1), phosphoserine phosphatase (PSPH) and GAPDH were designed using NCBI Primer-BLAST with melting temperatures between 58 and 63 °C, primer size between 18 and 30 base pairs and primers spanning across two exons.

NCBI accession number	Gene name	Direction	Sequence	Melting temperature (Tm)
NM_006623.3	PHGDH	Forward	5'GGGATGAAGACTATAGGGTATGAC'3	61
		Reverse	5'CAAAGGTGTTGTCATTCAGCAAG'3	
NM_058179.4	PSAT1	Forward	5'AGGATTCTACGTTTGTCCAGT'3	60
		Reverse	5'TGTGACAGCATTATACAGAGAGG'3	
NM_004577.3	PSPH	Forward	5'AAATCTGTGGCGTTGAGGAC'3	61
		Reverse	5'ACTTACCAGCTCCCTTATGC'3	
NM_001289745.3	GAPDH	Forward	5'CAGCCTCAAGATCATCAGCA'3	61
		Reverse	5'TGTGGTCATGAGTCCTTCCA'3	

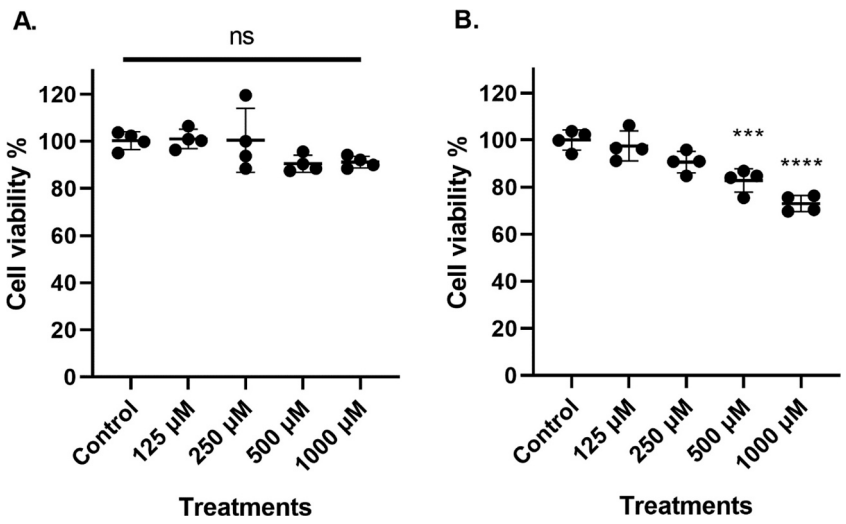

Fig. 1. Viability of SH-SY5Y neuroblastoma cells when treated with increasing concentrations of (A) BMAA and (B) 2,4-DAB for 48 h. Cell viability was compared to control cells (untreated) using the AlamarBlue® assay and normalised to cell protein. Statistical analysis using one-way ANOVA with Dunnett's multiple comparison test and plotted as mean ± SD. $^{**}P < 0.01$; ***P < 0.001; ****P < 0.0001; ns = non-significant ($n = 4$).

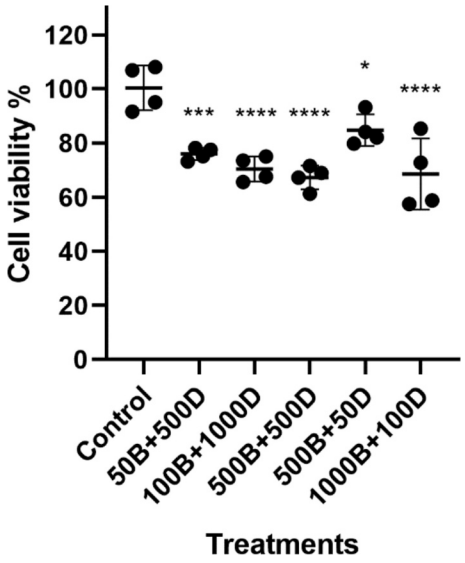

Fig. 2. Viability of SH-SY5Y neuroblastoma cells co-treated with a range of concentrations of BMAA (B) and 2,4-DAB (D) for 48 h. Cell viability was compared to the control cells (untreated) using the AlamarBlue® cell viability assay. Statistical analysis was carried out using one-way ANOVA with Dunnett's multiple comparison test and plotted as mean ± SD. $^{*}P < 0.05$; ***P < 0.001; $^{****}P < 0.0001$ (n = 4). Concentrations were 50 μM (50), 100 μM (100), 500 μM (500), and 1000 μM (1000).

3.3. Proteomic pathway analysis of SH-SY5Y neuroblastoma cells exposed to BMAA and 2,4-DAB

Approximately 3500 proteins were detected in cells that had been exposed to equimolar concentrations of BMAA (500 μM) and 2,4-DAB (500 μM) for 48 h. Differentially abundant proteins were identified if they were statistically significant (student *t*-test $p < 0.05$) and differed by at least ±30 % (FC > 1.3 or FC < 0.77) between control and treated cells. Out of 3500 proteins, 276 proteins were significantly altered in abundance (Fig. 3A). Heat map analysis of the differentially abundant proteins illustrated a consistent change in abundance of the proteins within the control and treatment groups (Fig. 3B). Statistical testing was based on the published method by Mirzaei (Mirzaei et al., 2017b). Ingenuity Pathways Analysis (IPA) identified a significant enrichment in pathways involved in L-serine biosynthesis ($p = 0.000071$) and energy production (fatty acid β-oxidation, $p = 0.000086$ and glycolysis, $p = 0.002$) (Fig. 3C).

IPA analysis of biological functions (Fig. 3D) identified an over-representation of proteins associated with neurological disorders, protein synthesis and degradation, mitochondrial dysfunction and cellular apoptosis.

3.4. Changes in expression of the enzymes in the L-serine biosynthesis pathway in cells incubated with BMAA and 2,4-DAB

Quantitative PCR was used to measure the expression of the three enzymes involved in the L-serine biosynthesis pathway. SH-SY5Y cells treated with 500 μM 2,4-DAB showed a significant decrease in PHGDH expression ($P < 0.01$) but BMAA did not have a significant effect at this concentration (Fig. 4A). Combined treatment with 500 μM BMAA with 500 μM 2,4-DAB resulted in a further decrease in PHGDH expression ($P < 0.0001$) (Fig. 4A). There was no significant change in the expression of the other two enzymes in the pathway, PSAT1 and PSPH, under the conditions tested (Fig. 4B and C).

3.5. Expression of PHGDH in SH-SY5Y cells treated with BMAA and 2,4-DAB is increased when the medium is supplemented with L-serine

We then examined if the BMAA and 2,4-DAB-induced decrease in expression of PHGDH was modulated by supplementation of the treatment media with L-serine. When SH-SY5Y cells were treated with 500 μM 2,4-DAB or 500 μM BMAA plus 500 μM 2,4-DAB, the expression of PHGDH was decreased by 35.2 % and 72.6 % respectively. The expression of PHGDH however, was restored to the same level as that in the 'control plus serine' treatment group for 2,4-DAB and BMAA plus 2,4-DAB-treated cells. L-serine was used at a ratio of 1:10 that of the NPAAs (50 μM and 100 μM respectively) (Fig. 5A).

3.6. Effect of L-serine on PSPH expression in SH-SY5Y cells treated with BMAA and 2,4-DAB

The final enzyme in the L-serine biosynthesis pathway (PSPH) is responsible for negative feedback in the presence of excess L-serine. In the control cells, the addition of L-serine resulted in a significant decrease in the level of expression of PSPH (Fig. 5B). The presence of 500 μM BMAA, or 500 μM 2,4-DAB, or 500 μM BMAA and 500 μM 2,4-

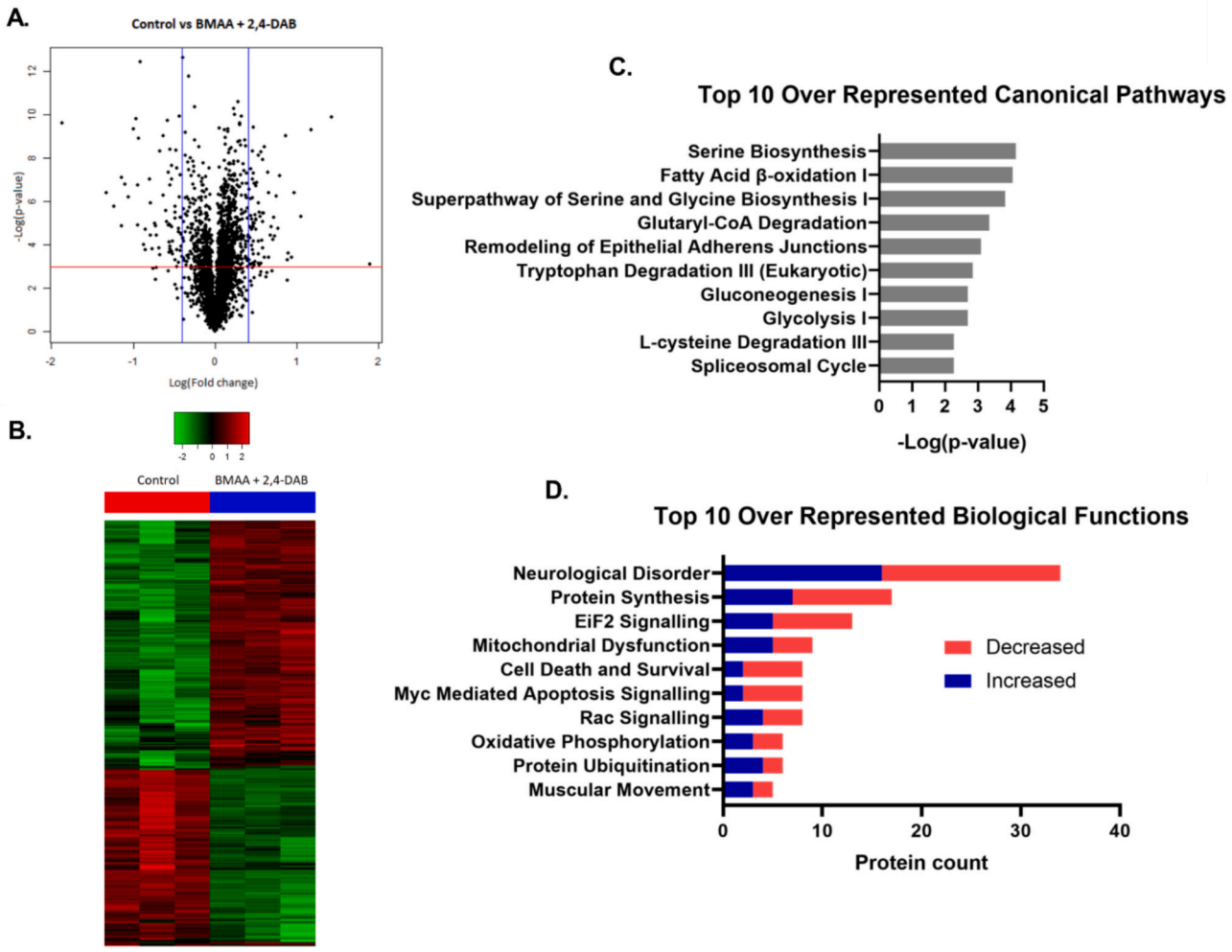

Fig. 3. (A) Volcano plot representation of protein abundance and significance in 500 μM BMAA plus 500 μM 2,4-DAB exposed cell cultures. Each dot represents a single quantified protein. An FC cut-off is applied at the 1.3 and 0.77 ratios (BMAA plus 2,4-DAB v control) and a significance cut-off is applied at $P < 0.05$. (B) Heat map of the log-transformed ratios of differentially abundant proteins. Green to red colour scale indicates relative decreases or increases in protein abundance respectively. (C) Top 10 most enriched canonical pathways identified by IPA functional analysis of differentially abundant proteins. Full table available under Supplementary Table 1. (D) Top 10 most enriched disease and biological functions as identified by IPA. (For interpretation of the references to colour in this figure legend, the reader is referred to the web version of this article.)

DAB had no impact on the decrease in expression of PSPH in the presence of L-serine.

3.7. Pre-treatment of SH-SY5Y cells with pyruvate prevented the decrease in expression of PHGDH enzyme in the presence of 2,4-DAB and 2,4-DAB and BMAA

SH-SY5Y cells were cultured in DMEM supplemented with pyruvate (0.11 g/L) before treatment with BMAA and 2,4-DAB as described previously (Fig. 4A). When cells were pre-treated with medium containing pyruvate there was no decrease in expression of PHGDH in response to 2,4-DAB as well as BMAA plus 2,4-DAB (Fig. 6).

3.8. Examination of PHGDH protein levels by western blotting

PHGDH protein levels were significantly decreased (63 %) in 500 μM BMAA plus 500 μM 2,4-DAB when compared to the untreated control (Fig. 7B).

4. Discussion

The gene-time-environment hypothesis posits that disease arises from the interaction of genetic burden and environmental insult over the course of a life (Al-Chalabi and Hardiman, 2013; McComas et al., 1973). Neurones being post-mitotic cells can accumulate damage over their lifespan (Drummond and Wilke, 2009) therefore for neurological diseases such as ALS, symptoms could develop after a threshold of neuronal damage is reached (Goutman et al., 2023). Epidemiological studies have identified clusters of ALS near water bodies with regular cyanobacterial blooms raising the possibility that long term exposure to cyanotoxins could contribute to a slow but continuous decline in motor neuron function leading eventually to cell death in genetically susceptible individuals (Caller et al., 2009; Caller et al., 2012). In the present studies we used SH-SY5Y neuroblastoma cells which lack NMDA receptors (Jantas et al., 2008; Kritis et al., 2015; Kulikov et al., 2007), thus the focus was not on acute, receptor-mediated toxicity as previously reported (Lobner et al., 2007; Schneider et al., 2020) but on investigating the impact that longer term exposure to the cyanotoxins BMAA and 2,4-DAB might have on the proteome. While 48 h cannot be equated with long-term exposure it allows a significant amount of protein synthesis and turnover to occur and allowed us to identify major changes in energy production in the cell.

Cellular health in the present studies was measured using AlamarBlue, a redox indicator that detects broad changes in enzyme

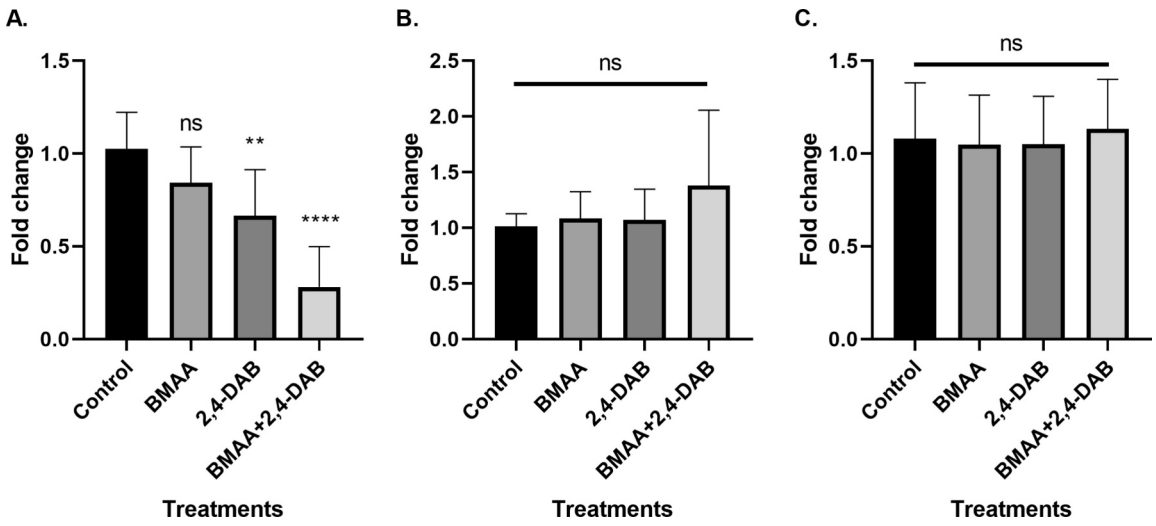

Fig. 4. PHGDH (A), PSAT1 (B) and PSPH (C) expression in SH-SY5Y neuroblastoma cells treated with 500 μM BMAA, 500 μM 2,4-DAB, and 500 μM BMAA plus 500 μM 2,4-DAB for 48 h. GAPDH was used as the housekeeping gene. The experiment was repeated three times on separate days for a total of $n = 9$. Fold change was calculated using the $2^{-\Delta\Delta CT}$ method (Livak and Schmittgen, 2001). Statistical analysis was performed using one-way ANOVA with Dunnett's multiple comparison test and plotted as mean ± SD. $^{**}P < 0.01$; $^{****}P < 0.0001$; ns = non-significant.

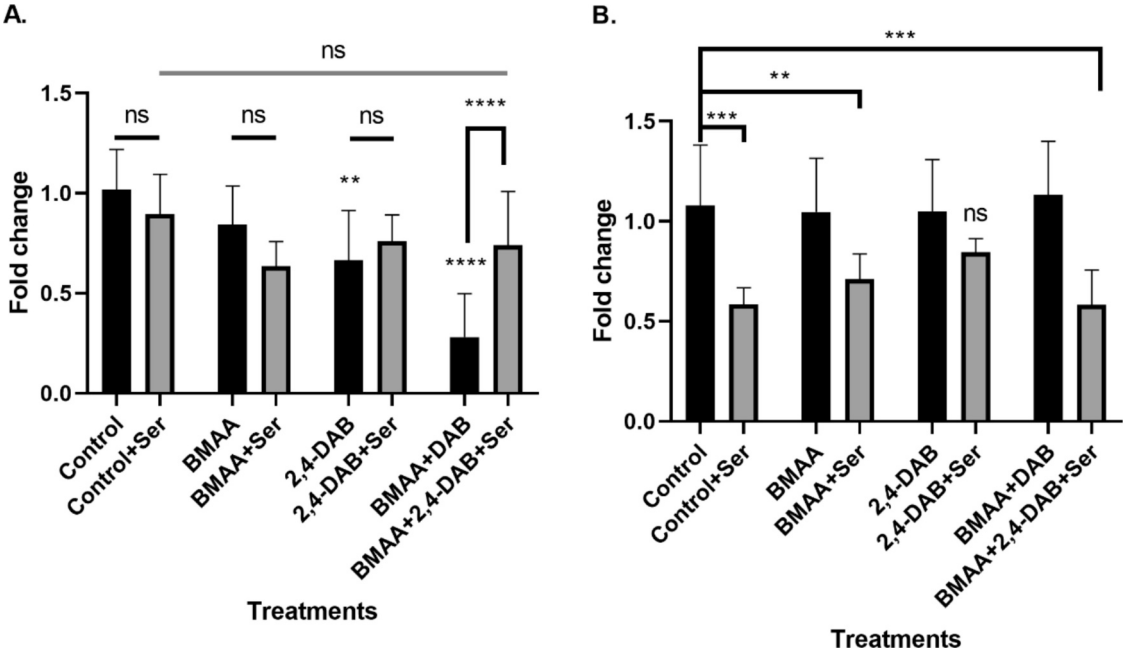

Fig. 5. PHGDH (A) and PSPH (B) expression in SH-SY5Y neuroblastoma cells treated for 48 h with 500 μM BMAA plus 50 μM L-serine; 500 μM 2,4-DAB plus 50 μM L-serine; 500 μM BMAA plus 500 μM 2,4-DAB plus 100 μM L-serine compared to the same conditions without L-serine. GAPDH was used as the housekeeping gene. Fold change was calculated using the $2^{-\Delta\Delta CT}$ method (Livak and Schmittgen, 2001). Statistical analysis was performed using one-way ANOVA with Sidak's multiple comparison test and plotted as mean ± SD. $^{**}P < 0.01$; $^{***}P < 0.001$; $^{****}P < 0.0001$; ns = non-significant (n = 9). Black significance represents significance relative to the control for each treatment, grey significance (top bar) represents significance relative to the control plus L-serine.

activity (Rampersad, 2012). DAB was significantly more toxic than its isomer BMAA (Fig. 1) suggesting that their mechanisms of toxicity differ. In support of this, combining two non-toxic concentrations of each, 50 μM DAB and 500 μM BMAA resulted in a significantly decreased cell viability indicating that they might have a joint effect. In addition, BMAA, despite not being significantly toxic to cells alone, increased the toxicity of 2,4-DAB so that concentrations of 2,4-DAB below 500 μM caused significant decreases in viability (Fig. 2).

Okle and colleagues, also using SH-SY5Y cells, reported that lower concentrations of BMAA resulted in disturbances in protein homeostasis and ER stress without the generation of reactive oxygen species and the significant levels of cell death that was seen at higher BMAA concentrations (Okle et al., 2013). In the present studies, pathway analysis of proteomic data identified disturbances in protein homeostasis in cells treated with BMAA and 2,4-DAB, with an increase in abundance of proteins involved in ubiquitination, and decreased levels of proteins required for the de-novo protein synthesis (Fig. 3D). We have previously shown BMAA alone damages proteins *in vitro* resulting in the accumulation of ubiquitin-positive aggregates (Quinn et al., 2021). BMAA was shown to increase neurofibrillary tangles and amyloid plaques in primate brains (Cox et al., 2016). Proteomic analysis identified an increase in caspase-3 protein, in cells following co-treatment with BMAA and 2,4-

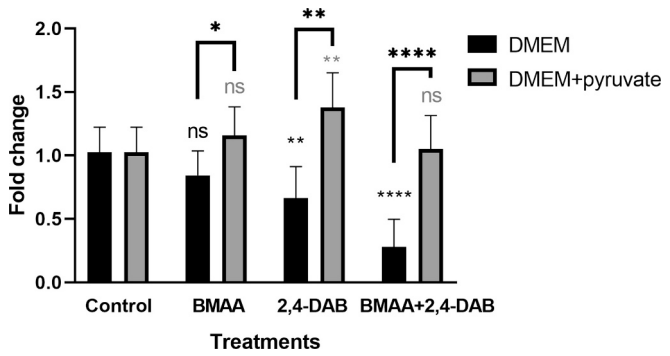

Fig. 6. PHGDH expression in SH-SY5Y neuroblastoma cells cultured medium with sodium pyruvate prior to treatment in medium containing 500 μM BMAA, 500 μM 2,4-DAB and 500 μM BMAA plus 500 μM 2,4-DAB for 48 h. GAPDH was used as the housekeeping gene. The experiment was repeated three times for a total of n = 9. Fold change was calculated using the $2^{-\Delta\Delta CT}$ method (Livak and Schmittgen, 2001). Statistical analysis was performed using one-way ANOVA with Sidak's multiple comparison test and plotted as mean ± SD. *$P < 0.05$; **P < 0.01; ****P < 0.0001; ns = non-significant. Black significance represents significance relative to the DMEM control, grey significance represents significance relative to the DMEM plus pyruvate control.

DAB suggesting that apoptotic cell death was increased. Our toxicity data is in general agreement with the simplex axial mixture study on zebrafish larval viability which reported that 2,4-DAB toxicity was greater than that of BMAA (Martin et al., 2022) and was consistent with the studies using mixed murine cortical cultures (Schneider et al., 2020).

Proteomic analysis revealed that L-serine biosynthesis was the most significantly impacted canonical pathway in cells exposed to BMAA and 2,4-DAB. This is of particular interest, given the established link between BMAA and L-serine (Bradley et al., 2018; Cox et al., 2016; Dunlop et al., 2013; Violi et al., 2023). The impact of BMAA and 2,4-DAB on the serine biosynthetic pathway was supported by demonstrating a significant decrease in the enzyme PHGDH at both mRNA and protein levels. This NAD^+-dependent enzyme is the first committed step in serine biosynthesis (Mullarky et al., 2016). 2,4-DAB alone also resulted in a significant decrease in PHGDH expression while BMAA caused a consistent but non-significant decrease in PHGDH expression. Only a single time point was evaluated in the present studies so the effect of BMAA on PHGDH expression is not clear, but BMAA was previously shown to cause a serine deficiency in cultured neuroblastoma cells (Violi et al., 2023). L-serine regulates the synthetic pathway through negative feedback on the expression of PSPH. Unlike L-serine, however BMAA and 2,4-DAB did not decrease the expression of PSPH (Fig. 5B) so do not act as L-serine 'mimics' through this feedback mechanism (de Koning et al., 2003).

Disturbances in the serine biosynthetic pathway by BMAA and 2,4-DAB could have important implications for neurological health due to the direct impact of serine deficiency on the CNS and also by promoting the synthesis of neurotoxic deoxysphingolipids (Esaki et al., 2015). L-serine plays an important role in the CNS as a precursor of the neuroactive substances, D-serine, and glycine (Metcalf et al., 2018). Interference with the L-serine synthesis might have important downstream effects since PHGDH deficiencies result in various neuropathologies (Jaeken et al., 1996). Humans with mutated PHGDH have lower levels of free L-serine in the plasma and cerebrospinal fluid and exhibit severe neurological symptoms, including congenital microcephaly, psychomotor retardation, and intractable seizures (de Koning and Klomp, 2004). PHGDH knock-out mice display severe consequences of embryonic development, such as brain malformation with overall growth retardation (Furuya et al., 2008). These human and mouse studies highlight the absolute necessity of L-serine, synthesised *de novo* for embryonic viability and nervous system development.

The *de novo* synthesis of sphingolipids (SLs) occurs in the endoplasmic reticulum from the serine palmitoyltransferase (SPT) catalysed

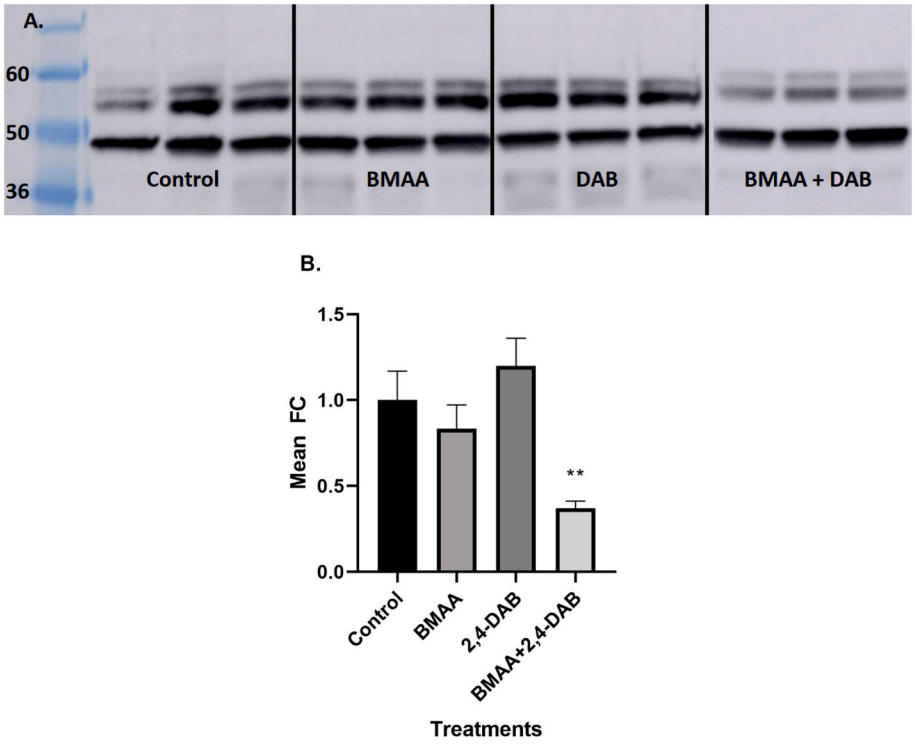

Fig. 7. PHGDH protein levels in SH-SY5Y cells were treated with 500 μM BMAA, 500 μM 2,4-DAB and 500 μM BMAA plus 500 μM 2,4-DAB for 48 h. 45 μg of protein was probed with a PHGDH antibody. Fig. 7A: A representative western blot of PHGDH (MW 57 kDa) and beta-actin (MW 41 kDa). Fig. 7B: Band density as was calculated using Amersham Imager 600 software and normalised to beta-actin. Statistical analysis was performed using one-way ANOVA with Dunnett's multiple comparison test and plotted as mean ± SD. **P < 0.01 ($n = 3$).

condensation of L-serine and acyl-CoA to produce 3-keto-dihydrosphingosine which is then processed into ceramide, the central molecule in the SL metabolic network (Pan et al., 2023). Complex sphingolipids such as sphingomyelin are synthesised from ceramide in the Golgi apparatus (Pan et al., 2023). A deficiency in L-serine can result in the synthesis of neurotoxic deoxysphingolipids (deoxySLs) due to a substrate shift from L-serine to L-alanine by SPT (Esaki et al., 2015). DeoxySLs differ structurally from canonical SLs and cannot be converted into complex sphingolipids (Pan et al., 2023). Elevated deoxySLs are implicated in several neurological diseases. Sera from patients with SPT-related hereditary sensory and autonomic neuropathy 1 (HSAN1), a disease that leads to progressive degeneration of motor neurons, have elevated levels of deoxySLs due to the substrate shift from L-serine to L-alanine (Mohassel et al., 2021). Elevated deoxySLs have also been reported in type 2 diabetes mellitus where they are thought to increase susceptibility to neuropathy (Dohrn et al., 2015). Disturbances in SL biosynthesis are a fundamental metabolic mechanism underlying the pathogenesis of ALS (Mohassel et al., 2021) and an abnormal increase in SL levels (sphingomyelin, ceramide, cholesterol, *etc.*) has been observed in the spinal cord of ALS patients, and in the spinal cord of SOD1G93A mice (Cutler et al., 2002). It is possible therefore that disturbances in serine biosynthesis in neuronal cells could contribute to the neurotoxic effects of the cyanotoxins BMAA and 2,4-DAB.

The major function of the serine biosynthesis pathway in proliferating cells is to maintain folate pools for nucleotide synthesis and to contribute to the glycine backbone of purines (Pacold et al., 2016). The activity of this pathway is critical even in the presence of excess exogenous serine since inhibition of this pathway results in the disruption of mass balance within central carbon metabolism leading to simultaneous alterations in the tricarboxylic acid (TCA) cycle and the pentose phosphate pathway (Reid et al., 2018). In the present studies, disturbances in serine biosynthesis were associated with significant changes in energy production pathways in BMAA and 2,4-DAB-treated cells: namely fatty acid β-oxidation, glycolysis, and oxidative phosphorylation, indicating that there was a significant disturbance in energy generation in the cells. Supplementation of the culture medium with pyruvate prior to exposure to BMAA and 2,4-DAB prevented the decrease in PHGDH expression. Pyruvate is the terminal metabolite of the glycolysis pathway which is linked to the L-serine biosynthesis pathway through the intermediate 3-phospho-D-glycerate (3PG) (Tabatabaie et al., 2010). Pyruvate is used as an additive in tissue culture media for its antioxidant properties and as an additional energy supplement. The presence of pyruvate might have provided an additional substrate for energy production *via* the TCA cycle potentially correcting the deficiency caused by 3PG being re-directed into the L-serine biosynthesis pathway.

Motor neurons have a low capacity for energy storage, and continual generation of ATP through the TCA cycle is required to meet their high energetic demands (Le Masson et al., 2014). Under energetic stress, by redirecting glucose from the pentose phosphate pathway (PPP) neurons sacrifice antioxidant production in favour of upregulating glycolysis (Rodriguez-Rodriguez et al., 2012; Stincone et al., 2015). Supplementation with pyruvate might have made additional substrates available allowing the TCA cycle to generate ATP without sacrificing glucose required for the PPP or serine biosynthesis pathway. The glycolytic pathway has previously been shown to be inhibited in zebrafish embryos exposed to 500 μM of 2,4-DAB for 4 days (Martin et al., 2022). Overall BMAA and 2,4-DAB appeared to cause a significant metabolic reprogramming in neuroblastoma cells *in vitro*. Metabolic profiling of serum from BMAA-treated neonatal rats identified systemic changes in amino acid metabolism and energy metabolism in neonates (Engskog et al., 2013). So while these neurotoxins might have a low neurotoxic potency in adults, exposure during development could cause long-term histopathological changes in the adult brain (Engskog et al., 2013).

5. Conclusions

In the present studies we examined changes in the proteome of human neuroblastoma cells following exposure to BMAA and 2,4-DAB, two cyanotoxins implicated in ALS. A key finding was impairment in the serine biosynthesis pathway. This is consistent with the findings of a study that demonstrated L-serine deficiency in BMAA-treated cells from direct analysis of intracellular amino acid levels (Violi et al., 2023). Serine deficiency has broad implications for neuronal health and could promote the synthesis of neurotoxic deoxysphingolipids due to a SPT substrate shift from serine to alanine (Esaki et al., 2015). In addition, there was evidence of energetic stress in BMAA and 2,4-DAB-treated cells which could make them more vulnerable to oxidants. Lastly, pretreatment of cells with pyruvate, the terminal metabolite in the glycolytic pathway, prevented the decrease in PHGDH expression potentially restoring the activity of the serine biosynthetic pathway. Pyruvate has been considered as a potential therapeutic for use in ALS (Vandoorne et al., 2018).

Authors Contribution

LP and KJR formulated research ideas. LP, CRP and JPV conducted the experiments. JRS contributed to proteomic results interpretation. LP and KJR analysed and interpreted the research work.

CRediT authorship contribution statement

Lisa Pu: Writing – original draft, Methodology, Formal analysis, Conceptualization. **Joel R. Steele:** Writing – review & editing, Methodology, Investigation. **Connor R. Phillips:** Writing – review & editing, Methodology, Investigation. **Jake P. Violi:** Writing – review & editing, Methodology, Investigation. **Kenneth J. Rodgers:** Writing – review & editing, Project administration, Methodology, Investigation, Conceptualization.

Ethical approval

Not applicable.

Funding

LP is a recipient of the Australian Government Research Training Program Stipend.

Declaration of competing interest

The authors declare the following financial interests/personal relationships which may be considered as potential competing interests:

Kenneth Rodgers has patent #US20130156846A1 United States issued to Kenneth Rodgers. If there are other authors, they declare that they have no known competing financial interests or personal relationships that could have appeared to influence the work reported in this paper.

Acknowledgements

The authors thank Dr. Mehdi Mirzaei from Macquarie University for running samples on the Orbitrap Fusion Tribrid-MS.

Appendix A. Supplementary data

Supplementary data to this article can be found online at https://doi.org/10.1016/j.tiv.2025.106058.

Data availability

All data are included as supplementary materials along with this publication.

Proteomic data generated from BMAA plus 2,4-DAB-treated cells were analysed using IPA. The full table of significantly enriched canonical pathways can be found below.

References

Al-Chalabi, A., Hardiman, O., 2013. The epidemiology of ALS: a conspiracy of genes, environment and time. Nat. Rev. Neurol. 9 (11), 617–628. https://doi.org/10.1038/nrneurol.2013.203.

Aranda, P.S., LaJoie, D.M., Jorcyk, C.L., 2012. Bleach gel: a simple agarose gel for analyzing RNA quality. Electrophoresis 33 (2), 366–369. https://doi.org/10.1002/elps.201100335.

Banack, S.A., Murch, S.J., 2009. Multiple neurotoxic items in the Chamorro diet link BMAA with ALS/PDC. Amyotroph. Lateral Scler. 10 (sup2), 34–40. https://doi.org/10.3109/17482960903278451.

Banack, S.A., Murch, S.J., Cox, P.A., 2006. Neurotoxic flying foxes as dietary items for the Chamorro people, Marianas Islands. J. Ethnopharmacol. 106 (1), 97–104. https://doi.org/10.1016/j.jep.2005.12.032.

Bradley, W.G., Miller, R.X., Levine, T.D., Stommel, E.W., Cox, P.A., 2018. Studies of environmental risk factors in amyotrophic lateral sclerosis (ALS) and a phase I clinical trial of l-serine. Neurotox. Res. 33 (1), 192–198. https://doi.org/10.1007/s12640-017-9741-x.

Büdel, B., Dulić, T., Darienko, T., Rybalka, N., Friedl, T., 2016. Cyanobacteria and algae of biological soil crusts. In: Weber, B., Büdel, B., Belnap, J. (Eds.), Biological Soil Crusts: An Organizing Principle in Drylands. Springer International Publishing, pp. 55–80. https://doi.org/10.1007/978-3-319-30214-0_4.

Cai, H.-Y., Tian, K.-W., Zhang, Y.-Y., Jiang, H., Han, S., 2018. Angiopoietin-1 and αvβ3 integrin peptide promote the therapeutic effects of L-serine in an amyotrophic lateral sclerosis/parkinsonism dementia complex model. Aging 10 (11), 3507–3527. https://doi.org/10.18632/aging.101661.

Caller, T.A., Doolin, J.W., Haney, J.F., Murby, A.J., West, K.G., Farrar, H.E., Ball, A., Harris, B.T., Stommel, E.W., 2009. A cluster of amyotrophic lateral sclerosis in New Hampshire: a possible role for toxic cyanobacteria blooms. Amyotroph. Lateral Scler. 10 (sup2), 101–108. https://doi.org/10.3109/17482960903278485.

Caller, T.A., Field, N.C., Chipman, J.W., Shi, X., Harris, B.T., Stommel, E.W., 2012. Spatial clustering of amyotrophic lateral sclerosis and the potential role of BMAA. Amyotroph. Lateral Scler. 13 (1), 25–32. https://doi.org/10.3109/17482968.2011.621436.

Cheng, R., Banack, S.A., 2009. Previous studies underestimate BMAA concentrations in cycad flour. Amyotroph. Lateral Scler. 10 (sup2), 41–43. https://doi.org/10.3109/17482960903273528.

Cox, P.A., Banack, S.A., Murch, S.J., 2003. Biomagnification of cyanobacterial neurotoxins and neurodegenerative disease among the Chamorro people of Guam. Proc. Natl. Acad. Sci. 100 (23), 13380–13383. https://doi.org/10.1073/pnas.2235808100.

Cox, P.A., Banack, S.A., Murch, S.J., Rasmussen, U., Tien, G., Bidigare, R.R., Metcalf, J.S., Morrison, L.F., Codd, G.A., Bergman, B., 2005. Diverse taxa of cyanobacteria produce β-N-methylamino-l-alanine, a neurotoxic amino acid. Proc. Natl. Acad. Sci. USA 102 (14), 5074–5078. https://doi.org/10.1073/pnas.0501526102.

Cox, P.A., Richer, R., Metcalf, J.S., Banack, S.A., Codd, G.A., Bradley, W.G., 2009. Cyanobacteria and BMAA exposure from desert dust: a possible link to sporadic ALS among gulf war veterans. Amyotroph. Lateral Scler. 10 (sup2), 109–117. https://doi.org/10.3109/17482960903286066.

Cox, P.A., Davis, D.A., Mash, D.C., Metcalf, J.S., Banack, S.A., 2016. Dietary exposure to an environmental toxin triggers neurofibrillary tangles and amyloid deposits in the brain. Proc. Biol. Sci. 283 (1823), 20152397. https://doi.org/10.1098/rspb.2015.2397.

Cutler, R.G., Pedersen, W.A., Camandola, S., Rothstein, J.D., Mattson, M.P., 2002. Evidence that accumulation of ceramides and cholesterol esters mediates oxidative stress-induced death of motor neurons in amyotrophic lateral sclerosis. Ann. Neurol. 52 (4), 448–457. https://doi.org/10.1002/ana.10312.

Davis, D.A., Cox, P.A., Banack, S.A., Lecusay, P.D., Garamszegi, S.P., Hagan, M.J., Powell, J.T., Metcalf, J.S., Palmour, R.M., Beierschmitt, A., Bradley, W.G., Mash, D. C., 2020. L-serine reduces spinal cord pathology in a Vervet model of preclinical ALS/MND. J. Neuropathol. Exp. Neurol. 79 (4), 393–406. https://doi.org/10.1093/jnen/nlaa002.

de Koning, T.J., Klomp, L.W., 2004. Serine-deficiency syndromes. Curr. Opin. Neurol. 17 (2), 197–204. https://journals.lww.com/co-neurology/Fulltext/2004/04000/Serine_deficiency_syndromes.19.aspx.

de Koning, T.J., Snell, K., Duran, M., Berger, R., Poll-The, B.-T., Surtees, R., 2003. L-serine in disease and development. Biochem. J. 371 (3), 653–661. https://doi.org/10.1042/bj20021785.

Dittmann, E., Fewer, D.P., Neilan, B.A., 2013. Cyanobacterial toxins: biosynthetic routes and evolutionary roots. FEMS Microbiol. Rev. 37 (1), 23–43. https://doi.org/10.1111/j.1574-6976.2012.12000.x.

Dohrn, M.F., Othman, A., Hirshman, S.K., Bode, H., Alecu, I., Fahndrich, E., Karges, W., Weis, J., Schulz, J.B., Hornemann, T., Claeys, K.G., 2015. Elevation of plasma 1-deoxy-sphingolipids in type 2 diabetes mellitus: a susceptibility to neuropathy? Eur. J. Neurol. 22 (5). https://doi.org/10.1111/ene.12663, 806-814, e855.

Drummond, D.A., Wilke, C.O., 2009. The evolutionary consequences of erroneous protein synthesis. Nat. Rev. Genet. 10 (10), 715–724. https://doi.org/10.1038/nrg2662.

Dunlop, R.A., Cox, P.A., Banack, S.A., Rodgers, K.J., 2013. The non-protein amino acid BMAA is Misincorporated into human proteins in place of l-serine causing protein Misfolding and aggregation. PLoS One 8 (9), e75376. https://doi.org/10.1371/journal.pone.0075376.

Eng, J.K., McCormack, A.L., Yates, J.R., 1994. An approach to correlate tandem mass spectral data of peptides with amino acid sequences in a protein database. J. Am. Soc. Mass Spectrom. 5 (11), 976–989. https://doi.org/10.1016/1044-0305(94)80016-2.

Engskog, M.K., Karlsson, O., Haglöf, J., Elmsjö, A., Brittebo, E., Arvidsson, T., Pettersson, C., 2013. The cyanobacterial amino acid β-N-methylamino-l-alanine perturbs the intermediary metabolism in neonatal rats. Toxicology 312, 6–11. https://doi.org/10.1016/j.tox.2013.07.010.

Esaki, K., Sayano, T., Sonoda, C., Akagi, T., Suzuki, T., Ogawa, T., Okamoto, M., Yoshikawa, T., Hirabayashi, Y., Furuya, S., 2015. L-serine deficiency elicits intracellular accumulation of cytotoxic Deoxysphingolipids and lipid body formation. J. Biol. Chem. 290 (23), 14595–14609. https://doi.org/10.1074/jbc.m114.603860.

Furuya, S., Yoshida, K., Kawakami, Y., Yang, J.H., Sayano, T., Azuma, N., Tanaka, H., Kuhara, S., Hirabayashi, Y., 2008. Inactivation of the 3-phosphoglycerate dehydrogenase gene in mice: changes in gene expression and associated regulatory networks resulting from serine deficiency. Funct. Integr. Genom. 8 (3), 235–249. https://doi.org/10.1007/s10142-007-0072-5.

Garruto, R.M., Gajdusek, D.C., Chen, K.M., 1981. Amyotrophic lateral sclerosis and parkinsonism-dementia among Filipino migrants to Guam. Ann. Neurol. 10 (4), 341–350. https://doi.org/10.1002/ana.410100405.

Goutman, S.A., Savelieff, M.G., Jang, D.G., Hur, J., Feldman, E.L., 2023. The Amyotrophic Lateral Sclerosis Exposome: Recent Advances and Future Directions. Nat. Rev. Neurol. https://doi.org/10.1038/s41582-023-00867-2.

Han, N.C., Bullwinkle, T.J., Loeb, K.F., Faull, K.F., Mohler, K., Rinehart, J., Ibba, M., 2020. The mechanism of beta-N-methylamino-l-alanine inhibition of tRNA aminoacylation and its impact on misincorporation. J. Biol. Chem. 295 (5), 1402–1410. https://doi.org/10.1074/jbc.RA119.011714.

Humphrey, S.J., Karayel, O., James, D.E., Mann, M., 2018. High-throughput and high-sensitivity phosphoproteomics with the EasyPhos platform. Nat. Protoc. 13 (9), 1897–1916. https://doi.org/10.1038/s41596-018-0014-9.

Huttlin, E.L., Ting, L., Bruckner, R.J., Gebreab, F., Gygi, M.P., Szpyt, J., Tam, S., Zarraga, G., Colby, G., Baltier, K., Dong, R., Guarani, V., Vaites, L.P., Ordureau, A., Rad, R., Erickson, B.K., Wühr, M., Chick, J., Zhai, B., Gygi, S.P., et al., 2015. The BioPlex network: a systematic exploration of the human Interactome. Cell 162 (2), 425–440. https://doi.org/10.1016/j.cell.2015.06.043.

Jaeken, J., Detheux, M., Van Maldergem, L., Frijns, J.P., Alliet, P., Foulon, M., Carchon, H., Van Schaftingen, E., 1996. 3-phosphoglycerate dehydrogenase deficiency and 3-phosphoserine phosphatase deficiency: inborn errors of serine biosynthesis. J. Inherit. Metab. Dis. 19 (2), 223–226. https://doi.org/10.1007/BF01799435.

Jantas, D., Pytel, M., Mozrzymas, J.W., Leskiewicz, M., Regulska, M., Antkiewicz-Michaluk, L., Lason, W., 2008. The attenuating effect of memantine on staurosporine-, salsolinol- and doxorubicin-induced apoptosis in human neuroblastoma SH-SY5Y cells. Neurochem. Int. 52 (4–5), 864–877. https://doi.org/10.1016/j.neuint.2007.10.003.

Kalhan, S.C., Hanson, R.W., 2012. Resurgence of serine: an often neglected but indispensable amino acid. J. Biol. Chem. 287 (24), 19786–19791. https://doi.org/10.1074/jbc.r112.357194.

Koreivienė, J., Anne, O., Fau-Kasperovičienė, J., Kasperovičienė, J., Fau-Burškytė, V., Burškytė, V., 2014. Cyanotoxin management and human health risk mitigation in recreational waters. Environ. Monit. Assess. 186 (7), 4443–4459. https://doi.org/10.1007/s10661-014-3710-0.

Kritis, A.A., Stamoula, E.G., Paniskaki, K.A., Vavilis, T.D., 2015. Researching glutamate–induced cytotoxicity in different cell lines: a comparative/collective analysis/study. Front. Cell. Neurosci. 9, 91. https://doi.org/10.3389/fncel.2015.00091.

Kulikov, A.V., Rzhaninova, A.A., Goldshtein, D.V., Boldyrev, A.A., 2007. Expression of NMDA receptors in multipotent stromal cells of human adipose tissue under conditions of retinoic acid-induced differentiation. Bull. Exp. Biol. Med. 144 (4), 626–629. https://doi.org/10.1007/s10517-007-0390-6.

Kurland, L.T., Mulder, D.W., 1954. Epidemiologic investigations of amyotrophic lateral sclerosis. I. Preliminary report on geographic distribution and special reference to the Mariana Islands, including clinical and pathologic observations. Neurology 4 (6), 438–448. https://doi.org/10.1212/wnl.4.6.438.

Le Masson, G., Przedborski, S., Abbott, L.F., 2014. A computational model of motor neuron degeneration. Neuron 83 (4), 975–988. https://doi.org/10.1016/j.neuron.2014.07.001.

Livak, K.J., Schmittgen, T.D., 2001. Analysis of relative gene expression data using real-time quantitative PCR and the 2−ΔΔCT method. Methods 25 (4), 402–408. https://doi.org/10.1006/meth.2001.1262.

Lobner, D., Piana, P.M.T., Salous, A.K., Peoples, R.W., 2007. β-N-methylamino-L-alanine enhances neurotoxicity through multiple mechanisms. Neurobiol. Dis. 25 (2), 360–366. https://doi.org/10.1016/j.nbd.2006.10.002.

Main, B.J., Rodgers, K.J., 2018. Assessing the combined toxicity of BMAA and its isomers 2,4-DAB and AEG in vitro using human neuroblastoma cells. Neurotox. Res. 33 (1), 33–42. https://doi.org/10.1007/s12640-017-9763-4.

Main, B.J., Dunlop, R.A., Rodgers, K.J., 2016. The use of l-serine to prevent β-methylamino-l-alanine (BMAA)-induced proteotoxic stress in vitro. Toxicon 109, 7–12. https://doi.org/10.1016/j.toxicon.2015.11.003.

Martin, R.M., Stallrich, J., Bereman, M.S., 2019. Mixture designs to investigate adverse effects upon co-exposure to environmental cyanotoxins. Toxicology 421, 74–83. https://doi.org/10.1016/j.tox.2019.04.013.

Martin, R.M., Bereman, M.S., Marsden, K.C., 2022. The cyanotoxin 2,4-DAB reduces viability and causes behavioral and molecular dysfunctions associated with neurodegeneration in larval zebrafish. Neurotox. Res. 40 (2), 347–364. https://doi.org/10.1007/s12640-021-00465-4.

McAlister, G.C., Huttlin, E.L., Haas, W., Ting, L., Jedrychowski, M.P., Rogers, J.C., Kuhn, K., Pike, I., Grothe, R.A., Blethrow, J.D., Gygi, S.P., 2012. Increasing the multiplexing capacity of TMTs using reporter ion isotopologues with isobaric masses. Anal. Chem. 84 (17), 7469–7478. https://doi.org/10.1021/ac301572t.

McAlister, G.C., Nusinow, D.P., Jedrychowski, M.P., Wühr, M., Huttlin, E.L., Erickson, B. K., Rad, R., Haas, W., Gygi, S.P., 2014. MultiNotch MS3 enables accurate, sensitive, and multiplexed detection of differential expression across cancer cell line proteomes. J. Anal. Chem. 86 (14), 7150–7158. https://doi.org/10.1021/ac502040v.

McComas, A.J., Upton, A.R., Sica, R.E., 1973. Motoneurone disease and ageing. Lancet 2 (7844), 1477–1480. https://doi.org/10.1016/s0140-6736(73)92735-9.

Metcalf, J.S., Dunlop, R.A., Powell, J.T., Banack, S.A., Cox, P.A., 2018. L-serine: a naturally-occurring amino acid with therapeutic potential. Neurotox. Res. 33 (1), 213–221. https://doi.org/10.1007/s12640-017-9814-x.

Mirzaei, M., Gupta, V.B., Chick, J.M., Greco, T.M., Wu, Y., Chitranshi, N., Wall, R.V., Hone, E., Deng, L., Dheer, Y., 2017a. Age-related neurodegenerative disease associated pathways identified in retinal and vitreous proteome from human glaucoma eyes. Sci. Rep. 7 (1), 12685. https://doi.org/10.1038/s41598-017-12858-7.

Mirzaei, M., Pascovici, D., Wu, J.X., Chick, J., Wu, Y., Cooke, B., Haynes, P., Molloy, M. P., 2017b. TMT one-stop shop: From reliable sample preparation to computational analysis platform. In: Keerthikumar, S., Mathivanan, S. (Eds.), Proteome Bioinformatics. Springer, New York, pp. 45–66. https://doi.org/10.1007/978-1-4939-6740-7_5.

Mohassel, P., Donkervoort, S., Lone, M.A., Nalls, M., Gable, K., Gupta, S.D., Foley, A.R., Hu, Y., Saute, J.A.M., Moreira, A.L., Kok, F., Introna, A., Logroscino, G., Grunseich, C., Nickolls, A.R., Pourshafie, N., Neuhaus, S.B., Saade, D., Gangfuss, A., Bonnemann, C.G., et al., 2021. Childhood amyotrophic lateral sclerosis caused by excess sphingolipid synthesis. Nat. Med. 27 (7), 1197–1204. https://doi.org/10.1038/s41591-021-01346-1.

Mullarky, E., Lucki, N.C., Beheshti Zavareh, R., Anglin, J.L., Gomes, A.P., Nicolay, B.N., Wong, J.C., Christen, S., Takahashi, H., Singh, P.K., Blenis, J., Warren, J.D., Fendt, S. M., Asara, J.M., DeNicola, G.M., Lyssiotis, C.A., Lairson, L.L., Cantley, L.C., 2016. Identification of a small molecule inhibitor of 3-phosphoglycerate dehydrogenase to target serine biosynthesis in cancers. Proc. Natl. Acad. Sci. USA 113 (7), 1778–1783. https://doi.org/10.1073/pnas.1521548113.

Okle, O., Stemmer, K., Deschl, U., Dietrich, D.R., 2013. L-BMAA induced ER stress and enhanced caspase 12 cleavage in human neuroblastoma SH-SY5Y cells at low Nonexcitotoxic concentrations. Toxicol. Sci. 131 (1), 217–224. https://doi.org/10.1093/toxsci/kfs291.

O'Neal, R.M., Chen, C.-H., Reynolds, C.S., Meghal, S.K., Koeppe, R.E., 1968. The 'neurotoxicity' of L-2,4-diaminobutyric acid. Biochem. J. 106 (3), 699–706. https://doi.org/10.1042/bj1060699.

Pacold, M.E., Brimacombe, K.R., Chan, S.H., Rohde, J.M., Lewis, C.A., Swier, L.J., Possemato, R., Chen, W.W., Sullivan, L.B., Fiske, B.P., Cho, S., Freinkman, E., Birsoy, K., Abu-Remaileh, M., Shaul, Y.D., Liu, C.M., Zhou, M., Koh, M.J., Chung, H., Sabatini, D.M., 2016. A PHGDH inhibitor reveals coordination of serine synthesis and one-carbon unit fate. Nat. Chem. Biol. 12 (6), 452–458. https://doi.org/10.1038/nchembio.2070.

Pan, X., Dutta, D., Lu, S., Bellen, H.J., 2023. Sphingolipids in neurodegenerative diseases. Front. Neurosci. 17, 1137893. https://doi.org/10.3389/fnins.2023.1137893.

Polsky, F.I., Nunn, P.B., Bell, E.A., 1972. Distribution and toxicity of alpha-amino-beta-methylaminopropionic acid. Fed. Proc. 31 (5), 1473–1475. https://www.ncbi.nlm.nih.gov/pubmed/5056173.

Quinn, A.W., Phillips, C.R., Violi, J.P., Steele, J.R., Johnson, M.S., Westerhausen, M.T., Rodgers, K.J., 2021. β-Methylamino-L-alanine-induced protein aggregation in vitro and protection by L-serine. Amino Acids 53 (9), 1351–1359. https://doi.org/10.1007/s00726-021-03049-w.

Rampersad, S.N.J.S., 2012. Multiple applications of Alamar blue as an indicator of metabolic function and cellular health in cell viability bioassays. Sensors 12 (9), 12347–12360. https://doi.org/10.3390/s120912347.

Reed, D., Plato, C., Elizan, T., Kurland, L.T., 1966. The amyotrophic lateral sclerosis/parkinsonism-dementia complex: a ten-year follow-up on Guam. I. Epidemiologic studies. Am. J. Epidemiol. 83 (1), 54–73. https://doi.org/10.1093/oxfordjournals.aje.a120570.

Reid, M.A., Allen, A.E., Liu, S., Liberti, M.V., Liu, P., Liu, X., Dai, Z., Gao, X., Wang, Q., Liu, Y., Lai, L.A.-O., Locasale, J.A.-O., 2018. Serine synthesis through PHGDH coordinates nucleotide levels by maintaining central carbon metabolism. Nat. Commun. 9 (1), 5442. https://doi.org/10.1038/s41467-018-07868-6.

Ressler, C., Redstone, P.A., Erenberg, R.H., 1961. Isolation and identification of a neuroactive factor from Lathyrus latifolius. Science 134 (3473), 188–190. https://doi.org/10.1126/science.134.3473.188.

Rodgers, K.J., Main, B.J., Samardzic, K., 2018. Cyanobacterial neurotoxins: their occurrence and mechanisms of toxicity. Neurotox. Res. 33 (1), 168–177. https://doi.org/10.1007/s12640-017-9757-2.

Rodriguez-Rodriguez, P., Fernandez, E., Almeida, A., Bolaños, J.P., 2012. Excitotoxic stimulus stabilizes PFKFB3 causing pentose-phosphate pathway to glycolysis switch and neurodegeneration. Cell Death Differ. 19 (10), 1582–1589. https://doi.org/10.1038/cdd.2012.33.

Schneider, T., Simpson, C., Desai, P., Tucker, M., Lobner, D., 2020. Neurotoxicity of isomers of the environmental toxin L-BMAA. Toxicon 184, 175–179. https://doi.org/10.1016/j.toxicon.2020.06.014.

Smith, Q.R., Momma, S., Aoyagi, M., Rapoport, S.I., 1987. Kinetics of neutral amino acid transport across the blood-brain barrier. J. Neurochem. 49 (5), 1651–1658. https://doi.org/10.1111/j.1471-4159.1987.tb01039.x.

Sompong, U., Hawkins, P.R., Besley, C., Peerapornpisal, Y., 2005. The distribution of cyanobacteria across physical and chemical gradients in hot springs in northern Thailand. FEMS Microbiol. Ecol. 52 (3), 365–376. https://doi.org/10.1016/j.femsec.2004.12.007.

Spencer, P.S., Hugon, J., Ludolph, A., Nunn, P.B., Ross, S.M., Roy, D.N., Schaumburg, H. H., 1987. Discovery and partial characterization of primate motor-system toxins. CIBA Found. Symp. 126, 221–238. https://doi.org/10.1002/9780470513422.ch14.

Stincone, A., Prigione, A., Cramer, T., Wamelink, M.M., Campbell, K., Cheung, E., Olin-Sandoval, V., Gruning, N.M., Kruger, A., Tauqeer Alam, M., Keller, M.A., Breitenbach, M., Brindle, K.M., Rabinowitz, J.D., Ralser, M., 2015. The return of metabolism: biochemistry and physiology of the pentose phosphate pathway. Biol. Rev. Camb. Philos. Soc. 90 (3), 927–963. https://doi.org/10.1111/brv.12140.

Tabatabaie, L., Klomp, L.W., Berger, R., de Koning, T.J., 2010. L-serine synthesis in the central nervous system: a review on serine deficiency disorders. Mol. Genet. Metab. 99 (3), 256–262. https://doi.org/10.1016/j.ymgme.2009.10.012.

Taton, A., Grubisic, S., Balthasart, P., Hodgson, D.A., Laybourn-Parry, J., Wilmotte, A., 2006. Biogeographical distribution and ecological ranges of benthic cyanobacteria in East Antarctic lakes. FEMS Microbiol. Ecol. 57 (2), 272–289. https://doi.org/10.1111/j.1574-6941.2006.00110.x.

Vandoorne, T., De Bock, K., Van Den Bosch, L., 2018. Energy metabolism in ALS: an underappreciated opportunity? Acta Neuropathol. 135 (4), 489–509. https://doi.org/10.1007/s00401-018-1835-x.

Violi, J.P., Mitrovic, S.M., Colville, A., Main, B.J., Rodgers, K.J., 2019. Prevalence of β-methylamino-L-alanine (BMAA) and its isomers in freshwater cyanobacteria isolated from eastern Australia. Ecotoxicol. Environ. Saf. 172, 72–81. https://doi.org/10.1016/j.ecoenv.2019.01.046.

Violi, J.P., Pu, L., Pravadali-Cekic, S., Bishop, D.P., Phillips, C.R., Rodgers, K.J., 2023. Effects of the toxic non-protein amino acid beta-Methylamino-L-Alanine (BMAA) on intracellular amino acid levels in neuroblastoma cells. Toxins (Basel) vol. 15 (11). https://doi.org/10.3390/toxins15110647.

Weiss, J.H., Christine, C.W., Choi, D.W., 1989. Bicarbonate dependence of glutamate receptor activation by β-N-methylamino-l-alanine: channel recording and study with related compounds. Neuron 3 (3), 321–326. https://doi.org/10.1016/0896-6273(89)90256-0.

Wessel, D., Flügge, U., 1984. A method for the quantitative recovery of protein in dilute solution in the presence of detergents and lipids. J. Anal. Biochem. 138 (1), 141–143. https://doi.org/10.1016/0003-2697(84)90782-6.

Whiting, M.G., 1963. Toxicity of cycads. Econ. Bot. 17 (4), 270–302. https://doi.org/10.1007/BF02860136.